

# ON THE POTENTIAL OF SIMPLE FRAMEWISE APPROACHES TO PIANO TRANSCRIPTION

Rainer Kelz, Matthias Dorfer, Filip Korzeniowski,  
Sebastian Böck, Andreas Arzt, Gerhard Widmer

Department of Computational Perception, Johannes Kepler University Linz, Austria  
rainer.kelz@jku.at

## ABSTRACT

In an attempt at exploring the limitations of simple approaches to the task of piano transcription (as usually defined in MIR), we conduct an in-depth analysis of neural network-based framewise transcription. We systematically compare different popular input representations for transcription systems to determine the ones most suitable for use with neural networks. Exploiting recent advances in training techniques and new regularizers, and taking into account hyper-parameter tuning, we show that it is possible, by simple bottom-up frame-wise processing, to obtain a piano transcriber that outperforms the current published state of the art on the publicly available MAPS dataset – without any complex post-processing steps. Thus, we propose this simple approach as a new baseline for this dataset, for future transcription research to build on and improve.

## 1. INTRODUCTION

Since their tremendous success in computer vision in recent years, neural networks have been used for a large variety of tasks in the audio, speech and music domain. They often achieve higher performance than hand-crafted feature extraction and classification pipelines [20]. Unfortunately, using this model class brings along considerable computational baggage in the form of hyper-parameter tuning. These hyper-parameters include architectural choices such as the number and width of layers and their type (e.g. dense, convolutional, recurrent), learning rate schedule, other parameters of the optimization scheme and regularizing mechanisms. Whereas for computer vision these successes were possible using raw pixels as the input representation, in the audio domain there seems to be an additional complication. Here the choices for how to best represent the input range from spectrograms, logarithmically filtered spectrograms over constant-Q transforms to even the raw audio itself [10].



© Rainer Kelz, Matthias Dorfer, Filip Korzeniowski, Sebastian Böck, Andreas Arzt, Gerhard Widmer. Licensed under a Creative Commons Attribution 4.0 International License (CC BY 4.0). **Attribution:** Rainer Kelz, Matthias Dorfer, Filip Korzeniowski, Sebastian Böck, Andreas Arzt, Gerhard Widmer. “On the Potential of Simple Framewise Approaches to Piano Transcription”, 17th International Society for Music Information Retrieval Conference, 2016.

This is a tedious problem, and there seem to be only two solutions to it: manual hyper-parameter selection, where a human expert tries to make decisions based on her past experience, or automatic hyper-parameter optimization as discussed in [4, 11, 28]. In this work we pursue a mixed strategy. As a first step, we systematically find the most suitable input representation, and progress from there with human expert knowledge to find best performing architectures for the task of framewise piano transcription.

A variety of neural network architectures has been used specifically for framewise transcription of piano notes from monaural sources. Some transcription systems are separated into an *acoustic model* and a *musical language model*, such as [7, 26, 27], whereas in others there is no such distinction [2, 6, 23]. As shown in [26], models that utilize *musical language models* perform better than those without, albeit the differences seem to be small. We focus on the *acoustic model* here, neglecting the complementary language model for now.

## 2. INPUT, METHODS AND PARAMETERS

In what follows, we will describe the input representations we compared, and give a brief overview of techniques for training and regularizing neural networks.

### 2.1 Input Representation

Time-frequency representations in the form of spectrograms still seem to have a distinct advantage over the raw audio input, as mentioned in [10]. The exact parameterization of spectrograms is not entirely clear however, so we try to address this question in a systematic way. We investigate the suitability of different types of spectrograms and constant-Q transforms as input representations for neural networks and compare four types of input representations: spectrograms with linearly spaced bins  $S$ , spectrograms with logarithmically spaced bins  $LS$ , spectrograms with logarithmically spaced bins and logarithmically scaled magnitude  $LM$ , as well as the constant-Q transform  $CQT$  [8]. The filterbank for  $LS$  and  $LM$  has a linear response (and lower resolution) for the lower frequencies, and a logarithmic response for the higher frequencies. We vary the sample rate  $sr \in \{22050, 44100\}$  [Hz], number of bands per octave  $nb \in \{12, 24, 36, 48\}$ , whether or not frames undergo circular shift  $cs \in \{\text{on}, \text{off}\}$ , the amount of zero padding  $zp \in \{\times 0, \times 1, \times 2\}$ , and whether or not

	<i>sr</i>	<i>zp</i>	<i>cs</i>	<i>nb</i>	<i>norm</i>
<i>CQT</i>	×			×	
<i>S</i>	×	×	×		
<i>LS</i>	×	×	×	×	×
<i>LM</i>	×	×	×	×	×

**Table 1:** For each spectrogram type, these are the parameters that were varied. See text for a description of the value ranges.

to use area normalized filters when filter banks are used  $norm \in \{\text{yes}, \text{no}\}$ . Furthermore, we re-scale the magnitudes of the spectrogram bins to be in the range  $[0, 1]$ . Table 1 specifies which parameters are varied for which input type. For the computation of spectrograms we used Madmom [5] and for the constant-Q transform we used the Yaaf library [21].

## 2.2 Model Class and Suitability

Formally, neural networks are functions with the structure

$$\begin{aligned} \text{net}_k(\mathbf{x}) &= \mathbf{W}_k f_{k-1}(\mathbf{x}) + \mathbf{b}_k \\ f_k(\mathbf{x}) &= \sigma_k(\text{net}_k(\mathbf{x})) \\ f_0(\mathbf{x}) &= \mathbf{x} \end{aligned}$$

where  $\mathbf{x} \in \mathbb{R}^{w_{in}}$ ,  $f_k : \mathbb{R}^{w_{k-1}} \rightarrow \mathbb{R}^{w_k}$ ,  $\sigma$  is any element-wise nonlinear function,  $\mathbf{W}_k$  is a matrix in  $\mathbb{R}^{w_k \times w_{k-1}}$  called the *weight matrix*, and  $\mathbf{b}_k \in \mathbb{R}^{w_k}$  is a vector called *bias*. The subscript  $k \in \{0, \dots, L\}$  is the index of the layer, with  $k = 0$  denoting the input layer.

Choosing a very narrow definition on purpose, what we mean by a *model class*  $F$  is a fixed number of layers  $L$ , a fixed number of layer widths  $\{w_0, \dots, w_L\}$  and fixed types of nonlinearities  $\{\sigma_0, \dots, \sigma_L\}$ . A *model* means an instance  $f$  from this class, defined by its weights alone. References to the whole collection of weights will be made with  $\Theta$ .

For the task of framewise piano transcription we define the *suitability* of an input representation in terms of the performance of a simple classifier on this task, when given exactly this input representation.

Assuming we can reliably mitigate the risk of overfitting, we would like to argue that this method of determining suitable input representations, and using them for models with higher capacity, is the best we can do, given a limited computational budget.

Using a low-variance, high-bias model class, the perceptron, also called *logistic regression* or *single-layer* neural network, we learn a *spectral template* per note. To test whether the results stemming from this analysis are really relevant for higher-variance, lower-bias model classes, we run the same set of experiments again, employing a multi layer perceptron with exactly one hidden layer, colloquially called a *shallow net*. This small extension already gives the network the possibility to learn a shared, distributed representation of the input. As we will see, this has a considerable effect on how suitability is judged.

## 2.3 Nonlinearities and Initialization

Common choices for nonlinearities include the *logistic function*  $\sigma(a) = \frac{1}{1+e^{-a}}$ , *hyperbolic tangent*  $\sigma(a) = \tanh a$ , and *rectified linear units (ReLU)*  $\sigma(a) = \max(0, a)$ . Nonlinearities are necessary to make neural networks universal function approximators [16]. According to [13, 15], using ReLUs as the nonlinearities in neural networks leads to better behaved gradients and faster convergence because they do not saturate.

Before training, the weight matrices are initialized randomly. The scale of this initialization is crucial and depends on the used nonlinearity as well as the number of weights contributing to the activation [13, 15]. Proper initialization plays an even bigger role when networks with more than one hidden layer are trained [31]. This is also important for the transcription setting we use, as the output layer of our networks uses the logistic function, which is prone to saturation effects. Thus we decided on using ReLUs throughout, initialized with a uniform distribution having a scale of  $\pm\sqrt{2} \cdot \sqrt{\frac{2}{w_{k-1}+w_k}}$ . For the last layer with the logistic nonlinearity, we omit the gain factor of  $\sqrt{2}$ , as advised in [13].

## 2.4 Weight Decay

To reduce overfitting and regularizing the network, different priors can be imposed on the network weights. Usually a Gaussian or Laplacian prior is chosen, corresponding to an  $L_2$  or  $L_1$  penalty term on connection weights, added to the cost function  $\mathcal{L}_{reg} = \mathcal{L} + \lambda \sum_k \|\text{vec}(\mathbf{W}_k)\|_{1/2}$  [25, 32], where  $\mathcal{L}$  is an arbitrary, unregularized cost function and  $\lambda$  governs the extent of regularization. Adding both of these penalty terms corresponds to a technique called *Elastic Net* [33]. It is pointed out in [1] that using  $L_2$  regularization plays a similar role as *early stopping* and thus might be omitted. An  $L_1$  penalty on the other hand leads to sparser weights, as it has a tendency to drive weights with irrelevant contributions to zero.

## 2.5 Dropout

Applying dropout to a layer zeroes out a fraction of the activations of a hidden layer of the network. For each training case, a different random fraction is dropped. This prevents units from co-adapting, and relying too much on each other's presence, as reasoned in [30]. Dropout increases robustness to noise, improves the generalization ability of networks and mitigates the risk of overfitting. Additionally dropout can be interpreted as model-averaging of exponentially many models [30].

## 2.6 Batch Normalization

Batch normalization [18] seeks to produce networks whose individual activations per layer are zero-mean and unit-variance. This is ensured by normalizing the activations for each mini-batch at each training step. This effectively limits how far the activation distribution can drift away from zero-mean, unit-variance during training. Not only

does this alleviate the need of the weights of the subsequent layer to adapt to a changing input distribution during training, it also keeps the nonlinearities from saturating and in turn speeds up training. It has additional regularizing effects, which become more apparent the more layers a network has. After training is stopped, the normalization is performed for each layer and for the whole training set.

## 2.7 Layer Types

We employ three different types of layer. Their respective functions can all be viewed as matrix expressions in the end, and thus can be made to fit into the framework described in Section 2.2. For the sake of readability, we simply describe their function in a procedural way.

A *dense layer* consists of a dense matrix - vector pair  $(\mathbf{W}, \mathbf{b})$  together with a nonlinearity. The input is transformed via this affine map, and then passed through a nonlinearity.

A *convolutional layer* consists of a number  $C_k$  of convolution kernels of a certain size  $\{(\mathbf{W}_c, \mathbf{b}_c)\}_{c=0}^{C_k}$  together with a non-linearity. The input is convolved with each convolution kernel, leading to  $C_k$  different feature maps to which the same nonlinearity is applied.

*Max pooling layers* are used in convolutional networks to provide a small amount of translational invariance. They select the units with maximal activation in a local neighborhood  $(w_t, w_f)$  in time and frequency in a feature map. This has beneficial effects, as it makes the transcriber invariant to small changes in tuning.

*Global average pooling* layers are used in all-convolutional networks to compute the mean value of feature maps.

## 2.8 Architectures

There is a fundamental choice between a network with all dense layers, a network with all convolutional layers, and a mixed approach, where usually the convolutional layers are the first ones after the input layer followed by dense layers. Pooling layers, batch normalization and dropout application are interleaved. For all networks we have to choose the number of layers, how many hidden units per layer to use and when to interleave a regularization layer. For convolutional networks we have to choose the number of filter kernels and their extent in time and frequency direction.

## 2.9 Networks for Framewise Polyphonic Piano Transcription

The output layer of all considered model classes has 88 units, in line with the playable notes on most modern pianos, and the output nonlinearity is the logistic function, whose output ranges lie in the interval  $[0, 1]$ .

The loss function being minimized is the frame- and element-wise applied *binary crossentropy*

$$\mathcal{L}_{bce}^{(t)}(\mathbf{y}_t, \hat{\mathbf{y}}_t) = -(\mathbf{y}_t \cdot \log(\hat{\mathbf{y}}_t) + (1 - \mathbf{y}_t) \cdot \log(1 - \hat{\mathbf{y}}_t))$$

where  $\hat{\mathbf{y}}_t = f_L(\mathbf{x}_t)$  is the output vector of the network, and  $\mathbf{y}_t$  the ground truth at time  $t$ . As the overall loss over the whole training set we take the mean

$$\mathcal{L} = \frac{1}{T} \sum_{t=1}^T \mathcal{L}_{bce}^{(t)}$$

For the purpose of computing the performance measures, the prediction of the network is thresholded to obtain a binary prediction  $\bar{\mathbf{y}}_t = \hat{\mathbf{y}}_t > 0.5$ .

## 2.10 Optimization

The simplest way to adapt the weights  $\Theta$  of the network to minimize the loss is to take a small step with length  $\alpha$  in the direction of steepest descent:

$$\Theta_{i+1} = \Theta_i - \alpha \cdot \frac{\partial \mathcal{L}}{\partial \Theta}$$

Computing the true gradient  $\frac{\partial \mathcal{L}}{\partial \Theta} = \frac{1}{T} \sum_{t=1}^T \frac{\partial \mathcal{L}_{bce}^{(t)}}{\partial \Theta}$  requires a sum over the length of the whole training set, and is computationally too costly. For this reason, the gradient is usually only approximated from an i.i.d. random sample of size  $M \ll T$ . This is called *mini-batch stochastic gradient descent*. There are several extensions to this general framework, such as *momentum* [24], *Nesterov momentum* [22] or *Adam* [19], which try to smooth the gradient estimate, correct small missteps or adapt the learning rate dynamically, respectively. Additionally we can set a *learning rate schedule* that controls the temporal evolution of the learning rate.

## 3. DATASET AND MEASURES

The computational experiments have been performed with the MAPS dataset [12]. It provides MIDI-aligned recordings of a variety of classical music pieces. They were rendered using different hi-quality piano sample patches, as well as real recordings from an upright Disklavier. This ensures clean annotation and therefore almost no label-noise. For all performance comparisons the following framewise measures on the validation set are used:

$$\begin{aligned} P &= \sum_{t=0}^{T-1} \frac{TP[t]}{TP[t] + FP[t]} \\ R &= \sum_{t=0}^{T-1} \frac{TP[t]}{TP[t] + FN[t]} \\ F_1 &= \frac{2 \cdot P \cdot R}{P + R} \end{aligned}$$

The train-test folds are those used in [26] which were published online<sup>1</sup>. For each fold, the validation set consists of 43 tracks randomly removed from the train set,

<sup>1</sup> <http://www.eecs.qmul.ac.uk/~sss31/TASLP/info.html>

deviating from the 26 used in [26], and leading to a division of 173-43-54 between the three sets. Note that the test sets are the *same*, and are referred to as *configuration I* in [26]. The exact splits for *configuration II* were not published. We had to choose them ourselves, using the same methodology, which has the additional constraint that *only recordings of the real piano* are used for testing, resulting in a division of 180-30-60. This constitutes a more realistic setting for piano transcription.

#### 4. ANALYSIS OF RELATIVE HYPER-PARAMETER IMPORTANCE

To identify and select an appropriate input representation and determine the most important hyper-parameters responsible for high transcription performance, a multi-stage study with subsequent *fANOVA* analysis was conducted, as described in [17]. This is similar in spirit to [14], albeit on a smaller scale.

##### 4.1 Types of Representation

To isolate the effects of different input representations on the performance of different model classes, only parameters for the spectrogram were varied according to Table 1. This leads to 204 distinct input representations. The hyper-parameters for the model class as well as the optimization scheme were held *fixed*. To make our estimates more robust, we conducted multiple runs for the same type of input.

The results for each model class are summarized in Table 2, containing the three most influential hyper-parameters and the percentage of variability in performance they are responsible for. The most important hyper-parameter for both model classes is the type of spectrogram used, followed by pairwise interactions. Please note that the numbers in the percentage column are mainly useful to judge the *relative* importance of the parameters. We will see these relative importances put into a larger context later on.

In Figure 1, we can see the mean performance attainable with different types of spectrograms for both model classes. The error bars indicate the standard deviation for the spread in performance, caused by the rest of the varied parameters. Surprisingly, the spectrogram with logarithmically spaced bins and logarithmically scaled magnitude, *LM*, enables the shallow net to perform best, even though it is a clear mismatch for logistic regression. The lower performance of the constant-Q transform was quite unexpected in both cases and warrants further investigation.

##### 4.2 Greater context

Attempting a full grid search on all possible input representation and model class hyper-parameters described in Section 2 to compute their *true* marginalized performance is computationally too costly. It is possible however to compute the *predicted* marginalized performance of a hyper-parameter efficiently from a smaller subsample of the space, as shown in [17]. All parameters are randomly

Model Class	Pct	Parameters
Logistic Regression	48.6%	Spectrogram Type
	16.9%	Spectrogram Type × Normed Area Filters
	10.4%	Spectrogram Type × Sample Rate
Shallow Net	68.4%	Spectrogram Type
	20.8%	Spectrogram Type × Sample Rate
	5.7%	Sample Rate

**Table 2:** The three most important parameters determining input representation for different model classes

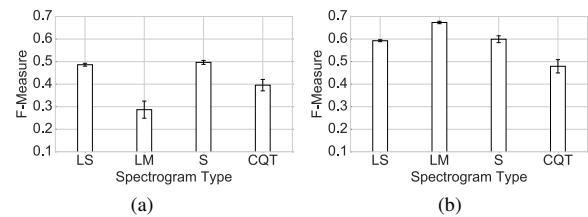


**Figure 1:** (a) Mean logistic regression performance dependent on spectrogram (b) Mean shallow net performance dependent on type of spectrogram

varied to sample the space as evenly as possible, and a random forest of 100 regression trees is fitted to the measured performance. This allows to *predict* the marginalized performance of individual hyper-parameters. Table 3 contains the list of hyper-parameters varied.

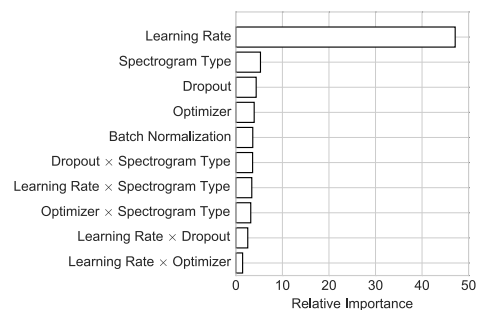


**Figure 2:** Relative importance of the first 10 hyper-parameters for the *shallow net* model class.

The percentage of variance in performance these hyper-parameters are responsible for, can be seen in Figure 2 for the 10 most important ones. A total of 3000 runs with random parameterizations were made.

Analyzing the results of all the runs tells us that the most important hyper-parameters are *Learning Rate* (47.11%), and *Spectrogram Type* (5.28%). The importance of the learning rate is in line with the findings in [14]. Figure 2 shows the relative importances of the first 10 hyper-parameters, and Figure 3 shows the predicted marginal performance of the learning rate dependent on its value (on a logarithmic scale) in greater detail.



Optimizer (Plain SGD, Momentum, Nesterov Momentum, Adam)  
 Learning Rate (0.001, 0.01, 0.1, 0.5, 1.0, 2.0, 10.0, 50.0, 100.0)  
 Momentum (Off, 0.7, 0.8, 0.9)  
 Learning rate Scheduler (On, Off)  
 Batch Normalization (On, Off)  
 Dropout (Off, 0.1, 0.3, 0.5)  
 $L_1$  Penalty (Off, 1e-07, 1e-08, 1e-09)  
 $L_2$  Penalty (Off, 1e-07, 1e-08, 1e-09)

**Table 3:** The list of additional hyper-parameters varied, and their ranges.

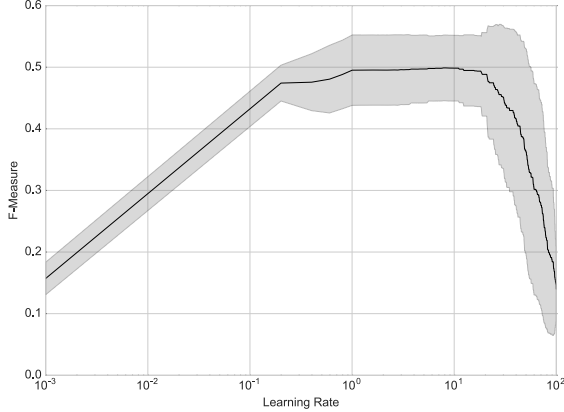


**Figure 3:** Mean predicted performance for the *shallow net* model class, dependent on learning rate (on a logarithmic scale). The dark line shows the mean performance, and the gray area shows the standard deviation.

## 5. STATE OF THE ART MODELS

Having completed the analysis of input representation, more powerful model classes were tried: a deep neural network consisting entirely of dense layers (*DNN*), a mixed network with convolutional layers directly after the input followed by dense layers (*ConvNet*), and an all-convolutional network (*AllConv* [29]). Their architectures are described in detail in Table 4. To the best of our knowledge, this is the first time an all-convolutional net has been proposed for the task of framewise piano transcription.

We computed a logarithmically filtered spectrogram with logarithmic magnitude from audio with a sample rate of 44.1 kHz, a filterbank with 48 bins per octave, normed area filters, no circular shift and no zero padding. The choices for circular shift and zero padding ranged very low on the importance scale, so we simply left them switched off. This resulted in only 229 bins, which are logarithmically spaced in the higher frequency regions, and almost linearly spaced in the lower frequency regions as mentioned in Section 2.1. The dense network was presented one frame at a time, whereas the convolutional network was given a context in time of two frames to either side of the current frame, summing to 5 frames in total.

All further hyper-parameter tuning and architectural choices have been left to a human expert. Models within a model class were selected based on average F-measure across the four validation sets. An automatic search via a hyper-parameter search algorithm for these larger model

	<i>DNN</i>	<i>ConvNet</i>	<i>AllConv</i>
	Input 229	Input 5x229	Input 5x229
	Dropout 0.1	Conv 32x3x3	Conv 32x3x3
	Dense 512	Conv 32x3x3	Conv 32x3x3
	BatchNorm	BatchNorm	BatchNorm
	Dropout 0.25	MaxPool 1x2	MaxPool 1x2
	Dense 512	Dropout 0.25	Dropout 0.25
	BatchNorm	Conv 64x3x3	Conv 32x1x3
	Dropout 0.25	MaxPool 1x2	BatchNorm
	Dense 512	Dropout 0.25	Conv 32x1x3
	BatchNorm	Dense 512	BatchNorm
	Dropout 0.25	Dropout 0.5	MaxPool 1x2
	Dense 88	Dense 88	Dropout 0.25
			Conv 64x1x25
			BatchNorm
			Conv 128x1x25
			BatchNorm
			Dropout 0.5
			Conv 88x1x1
			BatchNorm
			AvgPool 1x6
			Sigmoid
# Params	691288	1877880	284544

**Table 4:** Model Architectures

classes, as described in [4, 11, 28] is left for future work (the training time for a convolutional model is roughly 8–9 hours on a Tesla K40 GPU, which leaves us with 204.3–4.8 hours (variants  $\times$  #models  $\times$  #folds  $\times$  hours per model), or on the order of 800 – 900 days of compute time to determine the best input representation exactly).

For these powerful models, we followed practical recommendations for training neural networks via gradient descent found in [1]. Particularly relevant is the way of setting the initial learning rate. Strategies that dynamically adapt the learning rate, such as *Adam* or *Nesterov Momentum* [19, 22] help to a certain extent, but still do not spare us from tuning the initial learning rate and its schedule.

We observed that using a combination of batch normalization and dropout together with very simple optimization strategies leads to low validation error fairly quickly, in terms of the number of epochs trained. The strategy that worked best for determining the learning rate and its schedule was trying learning rates on a logarithmic scale, starting at 10.0, until the optimization did not diverge anymore [1], then training until the validation error flattened out for a few epochs, then multiplying the learning rate with a factor from the set {0.1, 0.25, 0.5, 0.75}. The rates and schedules we finally settled on were:

- *DNN*: SGD with Momentum,  $\alpha = 0.1$ ,  $\mu = 0.9$  and halving of  $\alpha$  every 10 epochs
- *ConvNet*: SGD with Momentum,  $\alpha = 0.1$ ,  $\mu = 0.9$  and a halving of  $\alpha$  every 5 epochs
- *AllConv*: SGD with Momentum,  $\alpha = 1.0$ ,  $\mu = 0.9$  and a halving of  $\alpha$  every 10 epochs

The results for framewise prediction on the MAPS dataset can be found in Table 6. It should be noted that we compare straightforward, simple, and largely un-smoothed

systems (ours) with hybrid systems [26]. There is a small degree of temporal smoothing happening when processing spectrograms with convolutional nets. The term *simple* is supposed to mean that the resulting models have a small amount of parameters and the models are composed of a few low-complexity building blocks. All systems are evaluated on the same train-test splits, referred to as *configuration I* in [26] as well as on *realistic* train-test splits, that were constructed in the same fashion as *configuration II* in [26].

Model Class	$P$	$R$	$F_1$
Hybrid DNN [26]	65.66	70.34	67.92
Hybrid RNN [26]	67.89	70.66	69.25
Hybrid ConvNet [26]	72.45	76.56	74.45
<b>DNN</b>	<b>76.63</b>	<b>70.12</b>	<b>73.11</b>
<i>ConvNet</i>	80.19	<b>78.66</b>	<b>79.33</b>
<i>AllConv</i>	<b>80.75</b>	75.77	78.07

**Table 5:** Results on the MAPS dataset. Test set performance was averaged across 4 folds as defined in *configuration I* in [26].

Model Class	$P$	$R$	$F_1$
DNN [26]	-	-	59.91
RNN [26]	-	-	57.67
ConvNet [26]	-	-	64.14
<i>DNN</i>	75.51	57.30	65.15
<i>ConvNet</i>	74.50	<b>67.10</b>	<b>70.60</b>
<i>AllConv</i>	<b>76.53</b>	63.46	69.38

**Table 6:** Results on the MAPS dataset. Test set performance was averaged across 4 folds as defined in *configuration II* in [26].

## 6. CONCLUSION

We argue that the results demonstrate: the importance of proper choice of input representation, and the importance of hyper-parameter tuning, especially the tuning of learning rate and its schedule; that convolutional networks have a distinct advantage over their deep and dense siblings, because of their context window and that all-convolutional networks perform nearly as well as mixed networks, although they have far fewer parameters. We propose these straightforward, framewise transcription networks as a new state-of-the-art baseline for framewise piano transcription for the MAPS dataset.

## 7. ACKNOWLEDGEMENTS

This work is supported by the European Research Council (ERC Grant Agreement 670035, project CON ESPRESSIONE), the Austrian Ministries BMVIT and BMWFW, the Province of Upper Austria (via the COMET Center SCCH) and the European Union Seventh Framework Programme FP7 / 2007-2013 through the GiantSteps project (grant agreement no. 610591). We would like to thank all developers of Theano [3] and Lasagne [9] for providing comprehensive and easy to use

deep learning frameworks. The Tesla K40 used for this research was donated by the NVIDIA Corporation.

## 8. REFERENCES

- [1] Yoshua Bengio. Practical recommendations for gradient-based training of deep architectures. In *Neural Networks: Tricks of the Trade*, pages 437–478. Springer, 2012.
- [2] Taylor Berg-Kirkpatrick, Jacob Andreas, and Dan Klein. Unsupervised Transcription of Piano Music. In *Advances in Neural Information Processing Systems*, pages 1538–1546, 2014.
- [3] James Bergstra, Olivier Breuleux, Frédéric Bastien, Pascal Lamblin, Razvan Pascanu, Guillaume Desjardins, Joseph Turian, David Warde-Farley, and Yoshua Bengio. Theano: a CPU and GPU Math Expression Compiler. In *Proceedings of the Python for Scientific Computing Conference (SciPy)*, 2010.
- [4] James Bergstra, Dan Yamins, and David D. Cox. Hyperopt: A python library for optimizing the hyperparameters of machine learning algorithms. In *Proceedings of the 12th Python in Science Conference*, pages 13–20, 2013.
- [5] Sebastian Böck, Filip Korzeniowski, Jan Schlüter, Florian Krebs, and Gerhard Widmer. madmom: a new Python Audio and Music Signal Processing Library. *arXiv preprint arXiv:1605.07008*, 2016.
- [6] Sebastian Böck and Markus Schedl. Polyphonic piano note transcription with recurrent neural networks. In *Acoustics, Speech and Signal Processing (ICASSP), 2012 IEEE International Conference on*, pages 121–124. IEEE, 2012.
- [7] Nicolas Boulanger-Lewandowski, Yoshua Bengio, and Pascal Vincent. Modeling temporal dependencies in high-dimensional sequences: Application to polyphonic music generation and transcription. *arXiv preprint arXiv:1206.6392*, 2012.
- [8] Judith C. Brown. Calculation of a constant Q spectral transform. *The Journal of the Acoustical Society of America*, 89(1):425–434, 1991.
- [9] Sander Dieleman, Jan Schlüter, Colin Raffel, Eben Olson, Søren Kaae Sønderby, Daniel Nouri, Daniel Mat-urana, Martin Thoma, Eric Battenberg, Jack Kelly, Jeffrey De Fauw, Michael Heilman, diogo149, Brian McFee, Hendrik Weideman, takacsg84, peterderivaz, Jon, instagibbs, Dr. Kashif Rasul, CongLiu, Britefury, and Jonas Degraive. Lasagne: First release., August 2015.
- [10] Sander Dieleman and Benjamin Schrauwen. End-to-end learning for music audio. In *Acoustics, Speech and Signal Processing (ICASSP), 2014 IEEE International Conference on*, pages 6964–6968. IEEE, 2014.

- [11] Katharina Eggensperger, Matthias Feurer, Frank Hutter, James Bergstra, Jasper Snoek, Holger Hoos, and Kevin Leyton-Brown. Towards an empirical foundation for assessing bayesian optimization of hyperparameters. In *NIPS workshop on Bayesian Optimization in Theory and Practice*, 2013.
- [12] Valentin Emiya, Roland Badeau, and Bertrand David. Multipitch estimation of piano sounds using a new probabilistic spectral smoothness principle. *Audio, Speech, and Language Processing, IEEE Transactions on*, 18(6):1643–1654, 2010.
- [13] Xavier Glorot and Yoshua Bengio. Understanding the difficulty of training deep feedforward neural networks. In *International Conference on Artificial Intelligence and Statistics*, pages 249–256, 2010.
- [14] Klaus Greff, Rupesh Kumar Srivastava, Jan Koutník, Bas R. Steunebrink, and Jürgen Schmidhuber. LSTM: A search space odyssey. *arXiv preprint arXiv:1503.04069*, 2015.
- [15] Kaiming He, Xiangyu Zhang, Shaoqing Ren, and Jian Sun. Delving Deep into Rectifiers: Surpassing Human-Level Performance on ImageNet Classification. *arXiv preprint arXiv:1502.01852*, 2015.
- [16] Kurt Hornik, Maxwell Stinchcombe, and Halbert White. Multilayer feedforward networks are universal approximators. *Neural networks*, 2(5):359–366, 1989.
- [17] Frank Hutter, Holger Hoos, and Kevin Leyton-Brown. An efficient approach for assessing hyperparameter importance. In *Proceedings of the 31st International Conference on Machine Learning (ICML-14)*, pages 754–762, 2014.
- [18] Sergey Ioffe and Christian Szegedy. Batch Normalization: Accelerating Deep Network Training by Reducing Internal Covariate shift. *arXiv preprint arXiv:1502.03167*, 2015.
- [19] Diederik Kingma and Jimmy Ba. Adam: A method for stochastic optimization. *arXiv preprint arXiv:1412.6980*, 2014.
- [20] Yann LeCun, Yoshua Bengio, and Geoffrey Hinton. Deep learning. *Nature*, 521(7553):436444, May 2015.
- [21] Benoit Mathieu, Slim Essid, Thomas Fillon, Jacques Prado, and Gaël Richard. YAAFE, an Easy to Use and Efficient Audio Feature Extraction Software. In *Proceedings of the International Conference on Music Information Retrieval*, pages 441–446, 2010.
- [22] Yurii Nesterov. A method of solving a convex programming problem with convergence rate  $O(1/k^2)$ . *Soviet Mathematics Doklady*, 27(2):372–376, 1983.
- [23] Ken O’Hanlon and Mark D. Plumbley. Polyphonic piano transcription using non-negative matrix factorisation with group sparsity. In *Acoustics, Speech and Signal Processing (ICASSP), 2014 IEEE International Conference on*, pages 3112–3116. IEEE, 2014.
- [24] Boris T. Polyak. Some methods of speeding up the convergence of iteration methods. *USSR Computational Mathematics and Mathematical Physics*, 4(5):1–17, 1964.
- [25] David E. Rumelhart, Geoffrey E. Hinton, and Ronald J. Williams. Learning representations by back-propagating errors. *Nature*, 323(6088), 1986.
- [26] Siddhartha Sigtia, Emmanouil Benetos, and Simon Dixon. An end-to-end neural network for polyphonic piano music transcription. *IEEE/ACM Transactions on Audio, Speech, and Language Processing*, 24(5):927–939, May 2016.
- [27] Siddhartha Sigtia, Emmanouil Benetos, Nicolas Boulanger-Lewandowski, Tillman Weyde, Artur S. d’Avila Garcez, and Simon Dixon. A hybrid recurrent neural network for music transcription. In *Acoustics, Speech and Signal Processing (ICASSP), 2015 IEEE International Conference on*, pages 2061–2065. IEEE, 2015.
- [28] Jasper Snoek, Hugo Larochelle, and Ryan P. Adams. Practical bayesian optimization of machine learning algorithms. In *Advances in neural information processing systems*, pages 2951–2959, 2012.
- [29] Jost Tobias Springenberg, Alexey Dosovitskiy, Thomas Brox, and Martin Riedmiller. Striving for Simplicity: The All Convolutional Net. *arXiv preprint arXiv:1412.6806*, 2014.
- [30] Nitish Srivastava, Geoffrey Hinton, Alex Krizhevsky, Ilya Sutskever, and Ruslan Salakhutdinov. Dropout: A simple way to prevent neural networks from overfitting. *The Journal of Machine Learning Research*, 15(1):1929–1958, 2014.
- [31] David Sussillo. Random Walks: Training Very Deep Nonlinear Feed-Forward Networks with Smart Initialization. *arXiv preprint arXiv:1412.6558*, 2014.
- [32] Peter M. Williams. Bayesian Regularization and Pruning Using a Laplace Prior. *Neural Computation*, 7(1):117–143, Jan 1995.
- [33] Hui Zou and Trevor Hastie. Regularization and variable selection via the elastic net. *Journal of the Royal Statistical Society: Series B (Statistical Methodology)*, 67(2):301–320, 2005.